

Solvent-Equilibrated Ion Pairs from Carbene Fragmentation Reactions

Robert A. Moss,* Fengmei Zheng, Jean-Marie Fedé, Lauren A. Johnson, and Ronald R. Sauers*

Contribution from the Department of Chemistry and Chemical Biology, Rutgers, The State University of New Jersey, New Brunswick, New Jersey 08903

Received May 24, 2004; E-mail: moss@rutchem.rutgers.edu

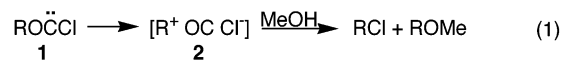
Abstract: $[R^+ OC Cl^-]$ ion pairs were generated in methanol/dichloroethane solutions, with R^+ as the 1-bicyclo[2.2.2]octyl, 1-adamantyl, or 3-homoadamantyl cation. Ion pairs were produced either by the *direct fragmentation* of alkoxychlorocarbenes (ROCCl), with $R = 1$ -bicyclo[2.2.2]octyl, 1-adamantyl, or 3-homoadamantyl, or by the *ring expansion–fragmentation* of $R'CH_2OCCl$, with $R' = 1$ -norbornyl, 3-noradamantyl, or 1-adamantyl. Correlations of the $[ROME]/[RCI]$ product ratios as a function of the mole fraction of MeOH in dichloroethane showed that the homoadamantyl chloride ion pairs, produced by either the direct or ring expansion–fragmentations, were identical, solvent- and anion-equilibrated, and precursor independent. Laser flash photolysis experiments gave 20–30 ps as the time required for solvent equilibration and precursor independence. Methanol/chloride selectivities of the (less-stable) 1-adamantyl chloride and 1-bicyclo[2.2.2]octyl chloride ion pairs were not independent of their ROCCl or $R'CH_2OCCl$ precursors. Computational studies provided transition states for the fragmentations and for the structures of the ion pairs.

Winstein's dissection¹ of the intermediates of solvolysis reactions into intimate ion pairs, solvent-separated ion pairs, and solvated ions has stood the test of time.² In some cases, picosecond laser flash photolysis, coupled with the deconvolution of complex kinetic behavior, permits the assignment of lifetimes to the several species and of rate constants to their interconversions. For example, the intimate (or contact) diphenylmethyl cation–chloride ion pair evolves to the solvent-separated ion pair in MeCN with $k = 2.87 \times 10^9 \text{ s}^{-1}$, in competition with internal return (collapse) to Ph_2CHCl with $k = 3.81 \times 10^9 \text{ s}^{-1}$.³ The lifetime of the contact ion pair is 150 ps.³ Rate constants governing the dynamics of the solvent-separated ion pair are also available.³

A related problem is the time required for the initial ion pair to become equilibrated with its solvent cage, thus permitting the counterion and solvent molecules to compete for the cation on the basis of comparative nucleophilicity and local concentration, and without specific 'memory' of the original precursor's structure. Here, we wish to describe a new method for the estimation of the time required for an ion pair to become solvent-equilibrated. Our method, which is based on carbene fragmentation chemistry, has two parts: First, we use product studies to

identify solvent-equilibrated ion pairs. Second, we use laser flash photolytic (LFP) methods to examine the dynamics of the ion pairs.

The fragmentations of certain alkoxychlorocarbenes (**1**) in polar solvents appear to proceed via ion pairs (**2**). In nucleophilic solvents such as methanol, these decay either by collapse to RCl or by solvolysis to ROME (eq 1).⁴ However, the fragmentation of ROCCl is a complicated process, capable of adopting different mechanisms depending on the structure of R and the polarity of the solvent.



We have encountered concerted fragmentation in nonpolar solvents,⁵ radical fragmentation in cryogenic matrixes⁵ or in the gas phase,⁶ and radical-like⁷ or anion-mediated S_N2 fragmentations⁸ when R cannot readily support a positive charge.

Now, we report that analyses of the product distributions from 'paired' fragmentations, in which nominally identical ion pairs form either directly or by ring expansion, allow us to identify those ion pairs that equilibrate with their solvent shell. Lifetime measurements then permit an estimate of the time required for this process. These results can also be associated with lifetimes of the ion pairs in the Winstein Scheme.^{1,2}

(1) Winstein, S.; Clippinger, E.; Fainberg, A. H.; Heck, R.; Robinson, G. C. *J. Am. Chem. Soc.* **1956**, *78*, 328.

(2) (a) Lowry, T. H.; Richardson, K. S. *Mechanism and Theory in Organic Chemistry*, 3rd ed.; New York: Harper & Row: 1987; pp 345f. (b) Carey, F. A.; Sundberg, R. J. *Advanced Organic Chemistry, Part A: Structure and Mechanisms*, 4th ed.; New York: Kluwer Academic/Plenum: 2000, pp 269f.

(3) Peters, K. S.; Li, B. *J. Phys. Chem.* **1994**, *98*, 401.

(4) Moss, R. A. *Acc. Chem. Res.* **1999**, *32*, 969.

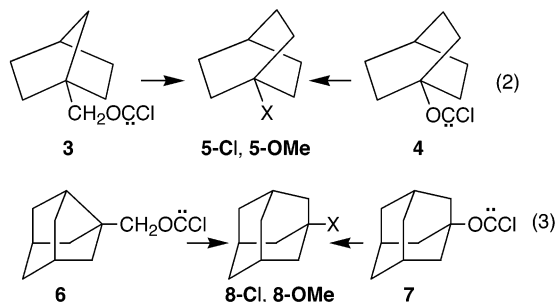
(5) Moss, R. A.; Ma, Y.; Zheng, F.; Sauers, R. R.; Bally, T.; Maltsev, A.; Toscano, J. P.; Showalter, B. M. *J. Phys. Chem. A* **2002**, *106*, 12280.

(6) Blake, M. E.; Jones, M., Jr.; Zheng, F.; Moss, R. A. *Tetrahedron Lett.* **2002**, *43*, 3069.

(7) Moss, R. A.; Ma, Y.; Sauers, R. R. *J. Am. Chem. Soc.* **2002**, *124*, 13968.

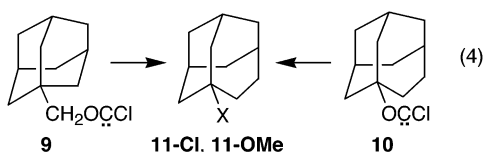
(8) Moss, R. A.; Johnson, L. A.; Merrer, D. C.; Lee, G. E., Jr. *J. Am. Chem. Soc.* **1999**, *121*, 5940.

Bridgehead carbocations can be generated directly by fragmentation of bridgehead ROCCl, or by ring-expanding rearrangement–fragmentation of appropriate RCH₂OCCl (cf., eqs 2 and 3).⁹ When the fragmentations of 1-norbornylmethoxy-



chlorocarbene (**3**) and 1-bicyclo[2.2.2]octyloxycarbene (**4**) occur in pure methanol, the ether/chloride product ratios [5-OMe]/[5-Cl] are *not* the same: 0.39 from **3** vs 2.5 from **4**.⁹ Clearly, identical, solvent-equilibrated ion pairs are not generated from both carbenes. Similarly, in pure methanol, 3-noradamantylmethoxycarbene (**6**) or 1-adamantylmethoxycarbene (**7**) afford different [8-OMe]/[8-Cl] product ratios: 0.43 from **6** vs 0.67 from **7**.⁹

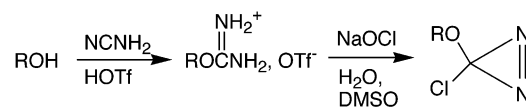
Can these differences be further narrowed or eliminated? The stability of bridgehead carbocations varies inversely with the structurally enforced deviation from planarity at the carbocation center.¹⁰ The relative gas-phase free energies of the 1-bicyclo[2.2.2]octyl, 1-adamantyl, and 3-homoadamantyl cations are −7.4, 0.0, and 4.2 kcal/mol, respectively.^{10a,11} The solution lifetimes of ion pairs **2** should be directly related to the stability of R⁺. Therefore, altering R⁺ from 1-adamantyl to the more stable 3-homoadamantyl cation should extend the ion pair lifetime. Here, we report that ion pairs with identical MeOH/Cl[−] selectivities, across the entire range of methanol–1,2-dichloroethane (DCE) compositions, form from either 1-adamantylmethoxycarbene (**9**) or 3-homo-1-adamantylmethoxycarbene (**10**) (eq 4).



Results and Discussion

Precursors and Products. The diazirine precursors for carbenes **3**,⁹ **4**,¹² **6**,⁹ **7**,¹² and **9**¹³ were available from previous studies. The precursor for carbene **10** was prepared from

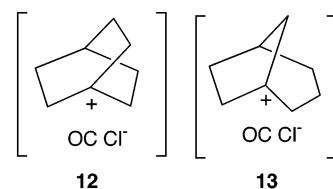
Scheme 1



3-homoadamantanol,¹⁴ which was converted to 3-homoadamantyl isouronium triflate with cyanamide and triflic acid.¹⁵ The latter was oxidized to 3-(3-homoadamantyl)-3-chlorodiazirine with NaOCl.¹⁶ The sequence is outlined in Scheme 1, and it was followed for all the other diazirine precursors, except for that of carbene **7**.¹²

Each carbene was photolytically generated from the appropriate 3-alkoxy-3-chlorodiazirine ($\lambda > 320$ nm, 25 °C) in MeOH/DCE at various mole fractions of MeOH. Products were identified by GC–MS, NMR, or GC comparisons with authentic samples. [ROMe]/[RCl] product ratios were determined by capillary GC.

From 1-norbornylmethoxycarbene (**3**), we obtained the products shown in Scheme 2.⁹ In pure MeOH, a typical product distribution (%) was **5-OMe** (10), **5-Cl** (26), **A** (1.3), **B** (3.1), **C** (30), **D** (14), and **E** (15); the [5-OMe]/[5-Cl] ratio was 0.39 ± 0.01 (mean of 2 runs). The simplest rationale for products **5-OMe** and **5-Cl** posits intermediate ion pair **12**, which arises by ring expansion–fragmentation of carbene **3**. The ion pair then gives the products by collapse with Cl[−] or capture by methanol. Below, we will refine our conception of the genesis of these products.



Products **D** and **E** similarly arise from ion pair **13**, which stems from the other possible ring expansion–fragmentation of **3**. As previously noted, expansion of the shorter, 1-carbon bridge of **3** exceeds expansion of the longer, 2-carbon bridge.⁹ Products **A–C** retain the structure of the initial carbene. The products **A** and **B** represent attack by methanol or chloride at the methylene group of **3**, whereas alcohol **C** is most reasonably construed as a carbene-trapping product: methanol captures about 30% of **3**, producing ROCH(Cl)OMe, which yields orthoformate ROCH(OMe)₂ and HCl by methanolysis. The orthoformate cannot be isolated; it returns alcohol **C** by acid-catalyzed hydrolysis with adventitious water.^{12,17}

Identification of products **A–E** is described by Moss et al.⁹ Authentic samples of key products **5-OMe** and **5-Cl** were obtained as follows. Chloride **5-Cl** was prepared from 1-norbornylmethanol,¹⁸ concentrated HCl, and ZnCl₂,¹⁹ which gave an 85:15 mixture of **5-Cl** and **E**. Ether **5-OMe** was obtained

- (9) Moss, R. A.; Zheng, F.; Fedé, J.-M.; Sauer, R. R. *Organic Lett.* **2002**, *4*, 2341.
 (10) (a) Abboud, J.-L. M.; Alkorta, I.; Davalos, J. Z.; Müller, P.; Quintanilla, E.; Rossier, J.-C. *J. Org. Chem.* **2003**, *68*, 3786. (b) Abboud, J.-L. M.; Herreros, M.; Notario, R.; Lomas, J. S.; Mareda, J.; Müller, P.; Rossier, J.-C. *J. Org. Chem.* **1999**, *64*, 6401. (c) Abboud, J.-L. M.; Alkorta, I.; Davalos, J. Z.; Müller, P.; Quintanilla, E. *Adv. Phys. Org. Chem.* **2002**, *37*, 57.
 (11) The values correspond to the relative free energies associated with chloride exchange between the 1-adamantyl cation and carbocation R⁺ in the gas phase, and afford a quantitative ranking of the intrinsic gas-phase stabilities of the carbocations.¹⁰
 (12) Moss, R. A.; Zheng, F.; Fedé, J.-M.; Ma, Y.; Sauer, R. R.; Toscano, J. P.; Showalter, B. M. *J. Am. Chem. Soc.* **2002**, *124*, 5258.
 (13) Moss, R. A.; Johnson, L. A.; Yan, S.; Toscano, J. P.; Showalter, B. M. *J. Am. Chem. Soc.* **2000**, *122*, 11256.

- (14) Farcasiu, D.; Jähme, J. Ruchardt, C. *J. Am. Chem. Soc.* **1985**, *107*, 5717.
 (15) Moss, R. A.; Kaczmarczyk, G. M.; Johnson, L.A. *Synth. Commun.* **2000**, *30*, 3233.
 (16) Graham, W. H. *J. Am. Chem. Soc.* **1965**, *87*, 4396.
 (17) Smith, N. P.; Stevens, I. D. R. *J. Chem. Soc., Perkin Trans. 2* **1979**, 1298. See, especially, pp 1302–1303.
 (18) Bixler, R. L.; Niemann, C. *J. Org. Chem.* **1958**, *23*, 742.
 (19) Kostova, K.; Dimitrov, V. *Synth. Commun.* **1995**, *25*, 1575.

Scheme 2

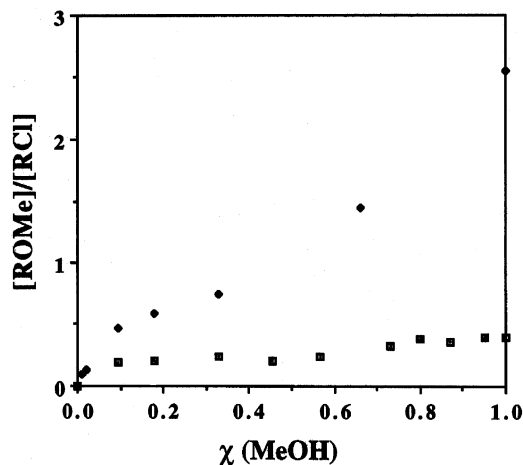
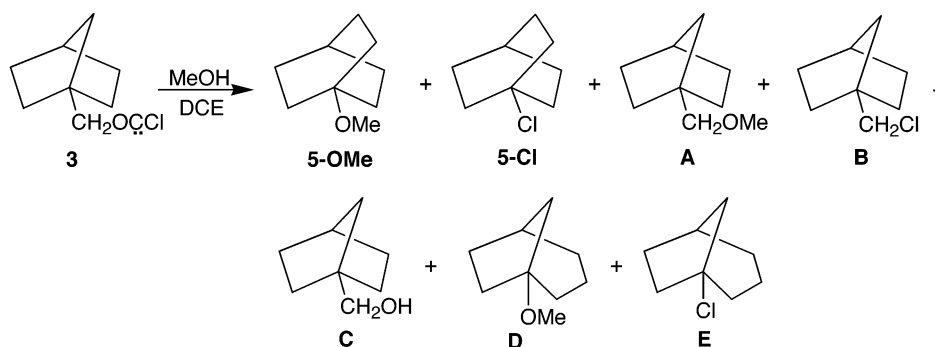
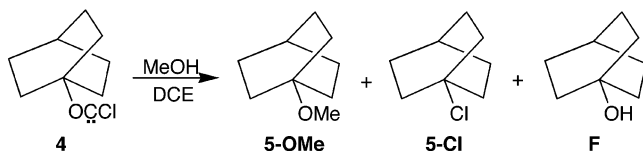


Figure 1. Product ratio [5-OMe]/[5-Cl] from the fragmentations of carbenes **3** (Scheme 2) and **4** (Scheme 3) in MeOH/DCE vs χ_{MeOH} (cf.; Tables S1 and S2 in the Supporting Information). Key: □ from carbene **3**, ◆ from carbene **4**.

Scheme 3



by the AgClO_4 -mediated methanolysis of 1-norbornylmethyl iodide.²⁰ Comparisons by GC, NMR, and MS verified product identities.

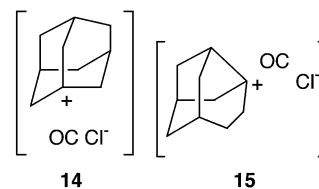
The dependence of the product ratio [5-OMe]/[5-Cl] on the mole fraction of MeOH in DCE appears in Figure 1. Table S1 in the Supporting Information collects distributions for all of the products in Scheme 2 at each of 11 MeOH mole fractions.

From 1-bicyclo[2.2.2]octyl chloroformate (**4**), we obtained the products shown in Scheme 3.¹² Products **5-OMe** and **5-Cl** stem from ion pair **12**, which here arises directly by the fragmentation of carbene **4**. The bicyclooctanol **F**^{18,19,21} may be regarded as the methanol capture product of **4**, which furnishes the alcohol after methanolysis and hydrolysis (see above, product **C**). In pure methanol, a typical distribution (%) is **5-OMe** (48), **5-Cl** (19), and **F** (32), with [5-OMe]/[5-Cl] = 2.52 ± 0.04 (mean of 2 runs). The dependence of the product ratio on the mole fraction of MeOH (in DCE) is shown in Figure 1. Distributions of the products in Scheme 3 at each of eight

methanol mole fractions are collected in Table S2 of the Supporting Information.

From 3-noradamantyl methoxychlorocarbene (**6**), we obtained the products shown in Scheme 4,⁹ which parallel those obtained from carbene **3** (cf., Scheme 2). In pure methanol, a typical product distribution (%) was **8-OMe** (16), **8-Cl** (35), **G** (12), **H** (9), **I** (1), **J** (25), **K** (2), while the [8-OMe]/[8-Cl] ratio was 0.43 ± 0.03 , (mean of 2 runs).

We suggest that products **8-OMe** and **8-Cl** come from ion pair **14**, formed by ring expansion–fragmentation of carbene **6**. The ion pair either collapses with its chloride counterion or is captured by methanol. Proadamantyl products **G** and **H** can be similarly rationalized, invoking ion pair **15**, which is formed by the alternative ring expansion–fragmentation of carbene **6**. As in the case of carbene **3**, ring expansion of the shorter (0-carbon) bridge of **6** exceeds expansion of its longer (1-carbon) bridge.⁹



Product **J** represents the methanol trapping product of carbene **6**, $\text{ROCH}(\text{Cl})\text{OMe}$, with subsequent methanolysis and hydrolysis. The formation of **J** from carbene **6** parallels the formation of alcohol **C** from carbene **3** (above). Identification of products **H**, **I**, and **J**²² is described by Moss et al.⁹ The identity of the protoadamantyl methyl ether (**G**) was assumed based on its MS molecular ion. An authentic sample of **8-OMe** was obtained from the AgClO_4 -mediated methanolysis of 1-adamantyl bromide,^{20,23} whereas authentic **8-Cl** was purchased from Aldrich. The product assignments in Scheme 4 were verified by GC–MS and GC spiking experiments.

The dependence of the product ratio [8-OMe]/[8-Cl] on the mole fraction of MeOH appears in Figure 2. Table S3 in the Supporting Information details the distribution of all the products of Scheme 4 at each of nine MeOH mole fractions in DCE.

From 1-adamantyl chloroformate (**7**), we obtained the products illustrated in Scheme 5.¹² Products **8-OMe** and **8-Cl** come from ion pair **14**, here formed directly by fragmentation of carbene **7**. The 1-adamantanol (**K**) represents the methanol/

(20) Kropp, P. J.; Poindexter, G. S.; Pienta, N. J.; Hamilton, D. C. *J. Am. Chem. Soc.* **1976**, *98*, 8135.

(21) Wiberg, K. B.; Lowry, B. R. *J. Am. Chem. Soc.* **1963**, *85*, 3188.

(22) (a) Tae, E. L.; Zhu, Z.; Platz, M. S. *J. Phys. Chem. A* **2001**, *105*, 3803. (b) Vogt, R. B.; Hoover, J. R. E. *Tetrahedron Lett.* **1967**, *8*, 2841. (c) Stoelting, D. T.; Shiner, V. J., Jr. *J. Am. Chem. Soc.* **1993**, *115*, 1695.

(23) Poindexter, G. S.; Kropp, P. J. *J. Org. Chem.* **1976**, *41*, 1215.

Scheme 4

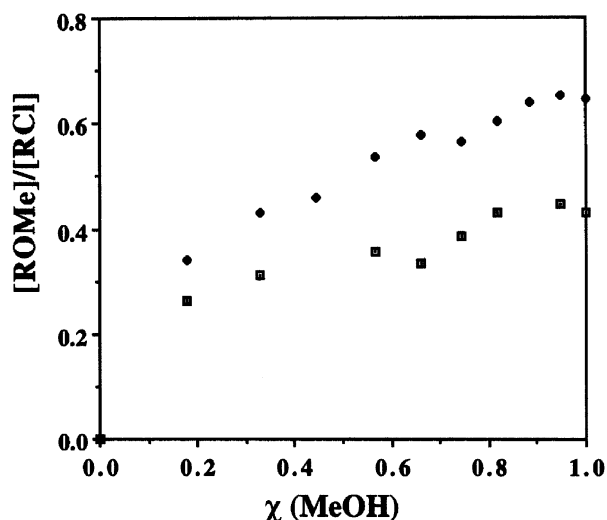
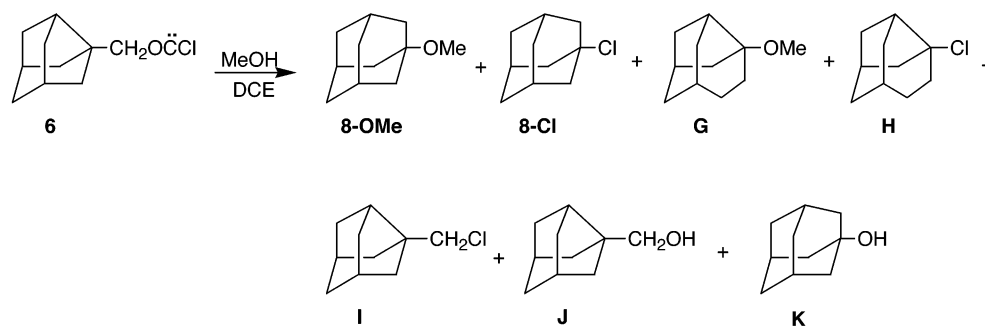


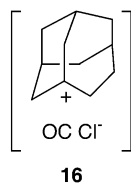
Figure 2. Product ratio [8-OMe]/[8-Cl] from the fragmentations of carbenes **6** (Scheme 4) and **7** (Scheme 5) in MeOH/DCE vs χ_{MeOH} (cf., Tables S3 and S4 in the Supporting Information). Key: \square from carbene **6**, \blacklozenge from carbene **7**.

carbene trapping—methanolysis/hydrolysis sequence that has been described above.

In pure methanol, a typical product distribution (%) is **8-OMe** (36), **8-Cl** (55), and **K** (9), with [8-OMe]/[8-Cl] = 0.67 ± 0.01 (mean of 2 runs). The dependence of the product ratio on the mole fraction of MeOH (in DCE) is shown in Figure 2; distributions of all of the products in Scheme 5, at each of 11 MeOH mole fractions, are collected in Table S4 of the Supporting Information.

From 1-adamantylmethoxychlorocarbene (**9**)¹³ we obtained the products shown in Scheme 6. In pure methanol, a typical product distribution (%) was **11-OMe** (23), **11-Cl** (35), **L** (not detected), **M** (42), and **N** (not detected). In pure DCE, we observed a distribution (%) of **L** (7.6), **N** (5.9), and **11-Cl** (86.5). In MeOH, the ratio [11-OMe]/[11-Cl] = 0.67 ± 0.01 (mean of 2 runs).

Products **11-Cl** and **11-OMe** are attributed to collapse or methanol capture of ion pair **16**, which arises from ring



expansion—fragmentation of carbene **9**. Products **M** and **N** represent capture of the carbene by methanol or water,²⁴ respectively. Product **L** stems from chloride attack on carbene **9** at its α -carbon.²⁴

The identity of **M** was secured by comparison with an authentic (commercial) sample. Chloride **L** was obtained from alcohol **M** and SOCl_2 ,²⁵ while formate **N** was prepared from **M** and formic acid, using $\text{BF}_3(\text{MeOH})_2$ as a catalyst.²⁶ For the key products, **11-OMe** and **11-Cl**, 3-homoadamantanol¹⁴ was first converted to **11-Cl** with SOCl_2 (reflux, 4 h).^{25,27} Chloride **11-Cl** could then be converted to **11-OMe** by refluxing with NaOMe/MeOH for 10 h. Both **11-Cl** and **11-OMe** were characterized by GC–MS, as well as ^1H and ^{13}C NMR spectroscopy. The reaction products in Scheme 6 were then verified by GC and GC–MS comparisons with the authentic samples.

The dependence of the product ratio [11-OMe]/[11-Cl] on the mole fraction of methanol is illustrated in Figure 3, while Table S5 in the Supporting Information collects the distributions of all of the products of Scheme 6 at each of 11 methanol mole fractions.

From 3-homoadamantylloxylchlorocarbene (**10**), we obtained the products shown in Scheme 7. Products **11-OMe** and **11-Cl** arise from ion pair **16**, formed here by the direct fragmentation of carbene **10**. The 3-homoadamantanol¹⁴ (**O**) derives from the methanol trapping/methanolysis/hydrolysis of carbene **10**.

In pure methanol, a typical product distribution (%) is **11-OMe** (27), **11-Cl** (36) and **O** (37), with [11-OMe]/[11-Cl] = 0.75 ± 0.01 (mean of 2 runs). The dependence of the product ratio on the mole fraction of methanol is shown in Figure 3, while distributions of the products in Scheme 7 at each of eight methanol mole fractions appear in Table S6 of the Supporting Information.

Dependence of Product Distributions on χ_{MeOH} . Inspection of Figures 1–3 reveals a dramatic evolution in correlations of the product ratio [ROME]/[RCI] with the mole fraction of methanol in the DCE solvent. Consider first eq 2, Schemes 2 and 3, and Figure 1. Here, [ROME]/[RCI] is strongly precursor dependent. From the fragmentation of carbene **4** (Scheme 3), [5-OMe]/[5-Cl] increases with χ_{MeOH} (Figure 1). This is in keeping with an ion pair intermediate, such as **12**, which can select between MeOH capture or chloride collapse, and which is responsive to methanol concentration. However, from the ring

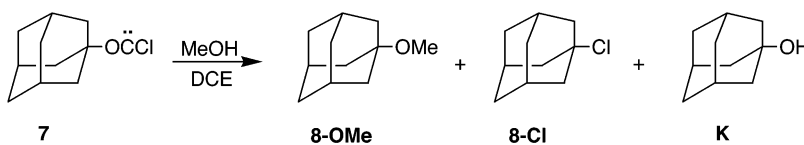
(24) Moss, R. A.; Ge, C.-S.; Maksimovic, L. *J. Am. Chem. Soc.* **1996**, *118*, 9792.

(25) Margosian, D.; Speier, J.; Kovacic, P. *J. Org. Chem.* **1981**, *46*, 136.

(26) Dymicky, M. *Org. Prep. Proced. Int.* **1982**, *14*, 177.

(27) Stetter, H.; Goebel, P. *Chem. Ber.* **1963**, *96*, 550.

Scheme 5



Scheme 6

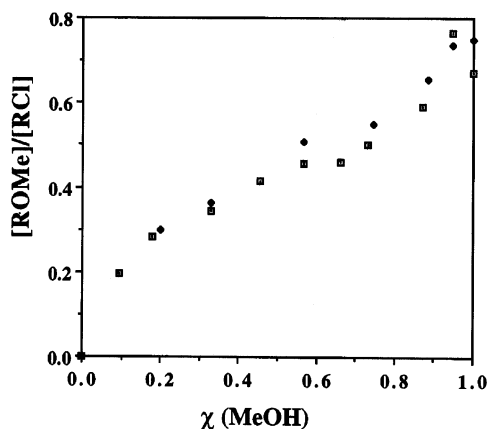
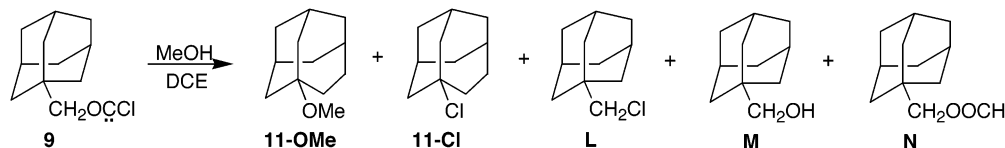
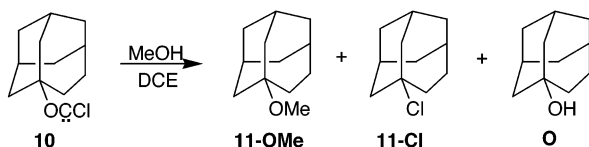


Figure 3. Product ratio [11-OMe]/[11-Cl] from the fragmentations of carbenes **9** (Scheme 6) and **10** (Scheme 7) in MeOH/DCE vs χ_{MeOH} (cf., Tables S5 and S6 in the Supporting Information). Key: \square from carbene **9**, \blacklozenge from carbene **10**.

Scheme 7



expansion–fragmentation of carbene **3** (Scheme 2), relatively little **5-OMe** forms; the dependence of [5-OMe]/[5-Cl] on χ_{MeOH} is nearly flat when $\chi_{\text{MeOH}} > 0.1$. At $\chi_{\text{MeOH}} = 1.0$, [5-OMe]/[5-Cl] is only ~ 0.4 , compared with ~ 2.5 from the direct fragmentation of carbene **4**. Clearly, the same ion pair (**12**) does not arise from both carbenes **3** and **4**, and the product-forming intermediate from **3** is certainly not a solvent-equilibrated ion pair.

In fact, computational studies (below) show that the conversion of carbene **3** to **5-Cl** transits a “tight” transition state that approximates the S_{Ni} mechanism. It is distinct from the ion pair arising in the fragmentation of carbene **4**, which more closely resembles the qualitative structure **12**.

Only a small component of the ring expansion–fragmentation of carbene **3** accesses ion pair **12** and ultimately yields **5-OMe**. Most of the fragmentation leads to **5-Cl** by a lower-energy, more “concerted” S_{Ni} -like transition state (see Figure 8a, below). We note that Jones et al.²⁸ suggested that certain alkoxychlorocarbenes fragment via S_{Ni} -like transition states, while Schleyer et

al.²⁹ provided experimental and computational evidence for an S_{Ni} -ion pair continuum in the decomposition of alkyl chlorosulfites, a reaction analogous to the fragmentation of alkoxychlorocarbenes.

In the 1-adamantyl ion pairs (**14**) obtained in the fragmentations of carbenes **6** and **7** (Schemes 4 and 5), the cation is more stable^{10,11} than the bicyclo[2.2.2]octyl cation obtained from carbenes **3** and **4**. Now, the ring expansion–fragmentation of carbene **6** more closely approaches the direct fragmentation of carbene **7** (Figure 2): [8-OMe]/[8-Cl] exhibits roughly parallel dependences on χ_{MeOH} from either carbene, and the mean final ratios in pure methanol, 0.43 from **6** and 0.67 from **7**, are not very widely separated.

Here, ion pair **14** is a reasonable qualitative representation of the product-forming intermediate from either carbene, and it is supported by computational studies (see below). The residual differences in [8-OMe]/[8-Cl] as a function of precursor suggest that the ion pairs, represented by **14**, approach, but do not quite achieve, equivalence. They cannot both be solvent equilibrated. (It is also possible that one ion pair, presumably from direct fragmentation of carbene **9** or direct fragmentation of carbene **7**, becomes solvent equilibrated, whereas the ion pair from ring expansion–fragmentation of carbene **6** does not reach that state.)

The even-more stable^{10,11} ion pairs **16**, however, achieve equivalence: within experimental error (± 0.04), the [11-OMe]/[11-Cl] ratios are very similar across the range of methanol mole fractions, and they are independent of their origin in either ring expansion–fragmentation of carbene **9** or direct fragmentation of carbene **10**, that is, “precursor amnesia” (cf., eq 4, Schemes 6 and 7, and Figure 3). These results constitute very strong evidence for counterion- and solvent-equilibrated ion pair **16** as the product determining intermediate in eq 4.

Computational Studies. A more-detailed structure for ion pair **16** is provided by DFT methodology. We first computed³⁰ the transition state for the fragmentation of 1-AdCH₂OCCl (**9**) (cf., Figure 4a).

We suggested,^{13,24} that the 1-AdCH₂OCCl fragmentation involved concerted ring expansion of the 1-AdCH₂ unit directly to the homoadamantyl cation. The B3LYP/6-31G(d) transition state (Figure 4a) supports this idea. Comparison of the ground-state bond lengths (in parentheses) with the corresponding transition-state bond lengths shows that the 1,2-carbon migration is in progress as the carbene fragments. Thus, the separation

(28) Likhovorik, I. R.; Jones, M., Jr.; Yurchenko, A. G.; Krasutsky, P. *Tetrahedron Lett.* **1989**, *30*, 5089.

(29) (a) Schreiner, P. R.; Schleyer, P. v. R.; Hill, R. K. *J. Org. Chem.* **1993**, *58*, 2822. (b) Schreiner, P. R.; Schleyer, P. v. R.; Hill, R. K. *J. Org. Chem.* **1994**, *59*, 1849.

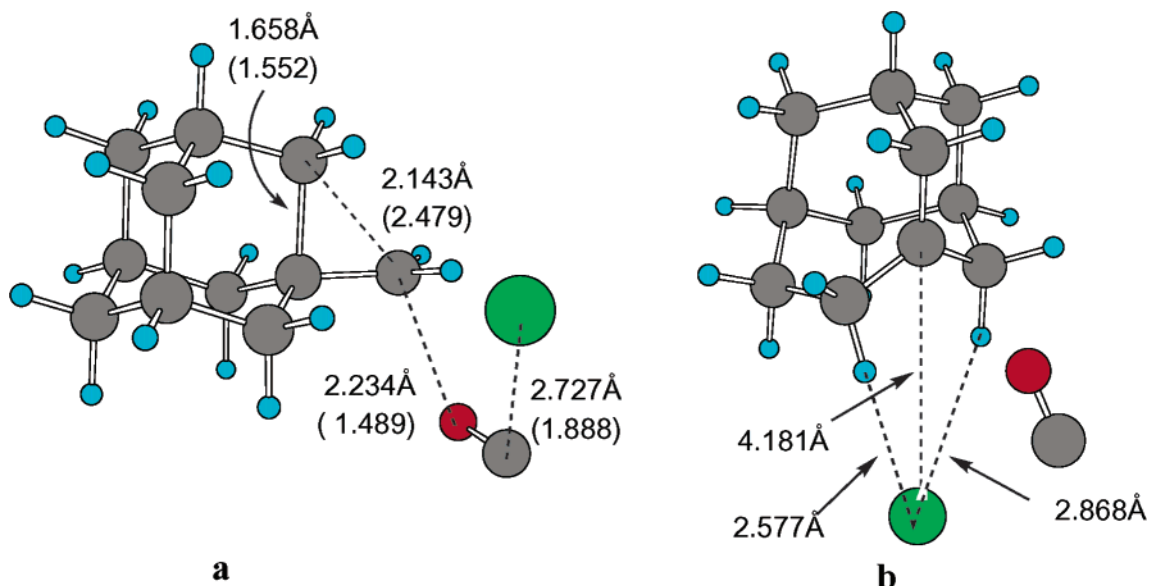


Figure 4. (a) B3LYP/6-31G(d) transition state for the ring expansion–fragmentation of carbene **9**. Bond lengths are shown for the TS and the carbene (in parentheses). ZPE and thermal corrections to 298 K have been applied. (b) Optimized ion pair from an intrinsic reaction coordinate calculation on the TS shown in (a), using B3LYP/6-31G(d) in simulated methanol with the polarized continuum model (PCM).³⁰ See the Computational Methodology section in the Experimental Section.

between the migrating CH₂ unit and the CH₂ migration terminus decreases from 2.479 to 2.143 Å, while the (breaking) bond between the migrant CH₂ and the tertiary carbon (C-3), which will become the cationic carbon in the homoadamantyl cation, increases from 1.552 to 1.658 Å. At the same time, the fragmenting C–O and C–Cl bonds increase from 1.489 to 2.234 Å and from 1.888 to 2.727 Å, respectively.

The transition state (TS) was then subjected to an intrinsic reaction coordinate (IRC) calculation affording an incipient ion pair (associated with CO) that was optimized in simulated methanol using the polarized continuum model (PCM). The resulting ion pair, shown in Figure 4b, displays apparent H-bonding between the chloride anion and protons on the carbon atoms that flank the cationic center. This feature undoubtedly contributes to the ion pair's existence in simulated methanol.

We believe this species to be a good approximation of the solvent-equilibrated ion pair formed by the ring expansion–fragmentation of carbene **9**, which was represented qualitatively as structure **16** (above).³¹ Moreover, given the small separation of the cation and chloride anion (4.18 Å in Figure 4b), we associate this ion pair with the intimate or contact ion pair of the Winstein solvolysis scheme.^{1,2}

Analogous computational studies of the fragmentation of 3-homoadamantylchlorocarbene (**10**) led to the TS depicted in Figure 5a. An IRC calculation afforded a structure that, when optimized in vacuo, gave homoadamantene by net elimination of HCl. However, no homoadamantene was detected in our solution experiments, and optimization of the computed transition structure in simulated methanol by the PCM procedure gave an ion pair (Figure 5b) that was essentially identical with that obtained from carbene **9** (Figure 4b). The computational studies thus support a mechanism in which solvent-equilibrated ion pairs **16** form from either carbene **9** or **10**, and display the identical Cl[−]/MeOH selectivity illustrated in Figure 3.

Computational analyses of the fragmentations of 3-noradamantylmethoxychlorocarbene (**6**) and 1-adamantylchlorocarbene (**7**) were similarly performed at the B3LYP/6-31G(d) level, affording the transition states depicted in Figure S1 (Supporting Information). For either carbene, IRC calculations, followed by optimization in simulated methanol (PCM), gave the same 1-adamantyl chloride ion pair (Figure 6). This species, rendered qualitatively as **14** (see above), resembles the 3-homoadamantyl chloride ion pair (**16**) obtained from carbenes **9** or **10** (Figures 4b and 5b); both have similar C⁺/Cl[−] separations, and both feature H-bonding of the chloride ion and ring protons.

Given the similarity of the ion pairs formed from carbenes **9** and **10**, or **6** and **7**, why do the former display identical Cl[−]/MeOH selectivity (Figure 3), whereas the latter do not (Figure 2)? ion pair lifetime must play the key role. Ion pair **16** from

(30) (a) Frisch, M. J.; Trucks, G. W.; Schlegel, H. B.; Scuseria, G. E.; Robb, M. A.; Cheeseman, J. R.; Zakrzewski, V. G.; Montgomery, J. A., Jr.; Stratmann, R. E.; Burant, J. C.; Dapprich, S.; Millam, J. M.; Daniels, A. D.; Kudin, K. N.; Strain, M. C.; Farkas, O.; Tomasi, J.; Barone, V.; Cossi, M.; Cammi, R.; Mennucci, B.; Pommelli, C.; Adamo, C.; Clifford, S.; Ochterski, J.; Petersson, G. A.; Ayala, P. Y.; Cui, Q.; Morokuma, K.; Malick, D. K.; Rabuck, A. D.; Raghavachari, K.; Foresman, J. B.; Cioslowski, J.; Ortiz, J. V.; Baboul, A. G.; Stefanov, B. B.; Liu, G.; Liashenko, A.; Piskorz, P.; Komaromi, I.; Gomperts, R.; Martin, R. L.; Fox, D. J.; Keith, T.; Al-Laham, M. A.; Peng, C. Y.; Nanayakkara, A.; Challacombe, M.; Gill, P. M. W.; Johnson, B. G.; Chen, W.; Wong, M. W.; Andres, J. L.; Gonzales, C.; Head-Gordon, M.; Repogle, E. S.; Pople, J. A. *Gaussian98*, Revision A9; Gaussian, Inc.: Pittsburgh, 1998. Frisch, M. J.; Trucks, G. W.; Schlegel, H. B.; Scuseria, G. E.; Robb, M. A.; Cheeseman, J. R.; Montgomery, J. A., Jr.; Vreven, T.; Kudin, K. N.; Burant, J. C.; Millam, J. M.; Iyengar, S. S.; Tomasi, J.; Barone, V.; Mennucci, B.; Cossi, M.; Scalmani, G.; Rega, N.; Petersson, G. A.; Nakatsuji, H.; Hada, M.; Ehara, M.; Toyota, K.; Fukuda, R.; Hasegawa, J.; Ishida, M.; Nakajima, T.; Honda, Y.; Kitao, O.; Nakai, H.; Klene, M.; Li, X.; Knox, J. E.; Hratchian, H. P.; Cross, J. B.; Adamo, C.; Jaramillo, J.; Gomperts, R.; Stratmann, R. E.; Yazyev, O.; Austin, A. J.; Cammi, R.; Piskorz, C.; Ochterski, J. W.; Ayala, P. Y.; Morokuma, K.; Voth, G. A.; Salvador, P.; Dannenberg, J. J.; Zakrzewski, V. G.; Dapprich, S.; Daniels, A. D.; Strain, M. C.; Farkas, O.; Malick, D. K.; Rabuck, A. D.; Raghavachari, K.; Foresman, J. B.; Ortiz, J. V.; Cui, Q.; Baboul, A. G.; Clifford, S.; Cioslowski, J.; Stefanov, B. B.; Liu, G.; Liashenko, A.; Piskorz, P.; Komaromi, I.; Martin, R. L.; Fox, D. J.; Keith, T.; Al-Laham, M. A.; Peng, C. Y.; Nanayakkara, A.; Challacombe, M.; Gill, P. M. W.; Johnson, B.; Chen, W.; Wong, M. W.; Gonzalez, C.; Pople, J. A. *Gaussian03*, Revision B.02; Gaussian, Inc.: Pittsburgh, 2003. (b) Becke, A. D. *J. Chem. Phys.* **1993**, *98*, 5648. (c) Lee, C.; Yang, W.; Parr, R. G. *Phys. Rev. B* **1988**, *37*, 785.

(31) The computed E_a for the fragmentation of **9** in simulated MeCN at the B3LYP/6-31G* level is 5.4 kcal/mol, in decent agreement with the measured value of 3.6 kcal/mol.¹³

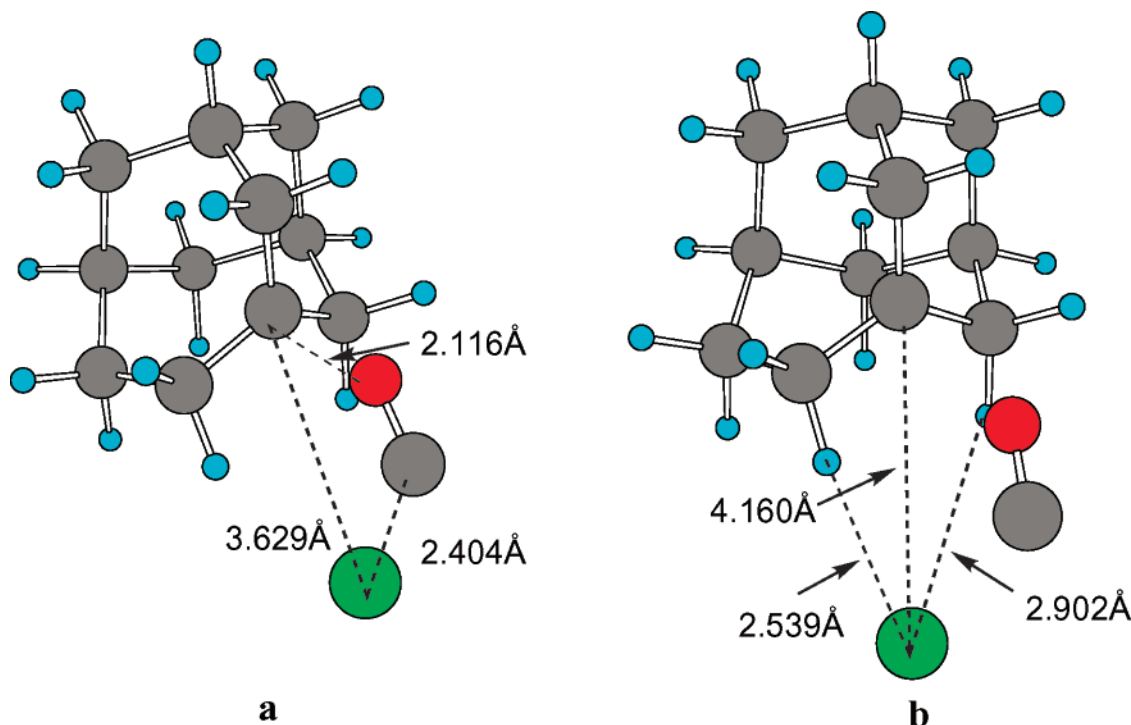


Figure 5. (a) B3LYP/6-31G(d) transition state for the fragmentation of carbene **10**. (b) Optimized ion pair from an IRC calculation on the TS shown in (a), using B3LYP/6-31G(d) in simulated methanol with the PCM.³⁰ See the Computational Methodology section in the Experimental Section.

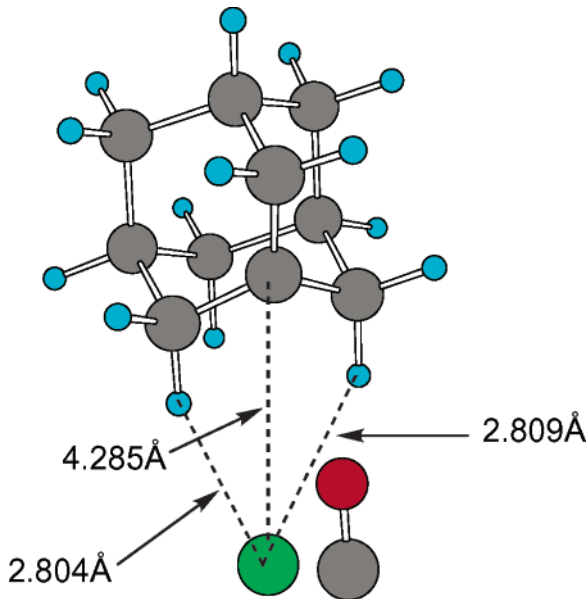


Figure 6. Optimized ion pair resulting from the ring expansion-fragmentation of carbene **6** or the fragmentation of carbene **7**, deriving from IRC calculations on the transition states shown in Figure S1 (Supporting Information), and using B3LYP/6-31G(d) in simulated methanol with the PCM.³⁰ See the Computational Methodology section in the Experimental Section.

carbenes **9** or **10** contains the more stable¹⁰ homoadamantyl cation and lives longer than the adamantyl chloride ion pair **14** from carbenes **6** or **7**, which permits equilibration of the former ion pair relative to its solvent cage. Ion pair **16** thus becomes independent of its precursor carbene. This is not true of ion pair **14**. With its less-stable cation and shorter lifetime, it evidently retains some “memory” of its precursor carbene.^{32,33} Below, we will estimate the time required for ion pair–solvent equilibration.

Computational studies of 1-norbornylmethoxychlorocarbene (**3**) and 1-bicyclo[2.2.2]oxychlorocarbene (**4**) are particularly interesting. The TS for fragmentation of carbene **4** (Figure 7a) leads, after IRC calculation and optimization in simulated methanol (PCM), to the ion pair (**12**) shown in Figure 7b. However, ring expansion–fragmentation of carbene **3** accesses two transition states (cf., Figure 8). The lower-energy TS (Figure 8a, $\Delta H_{\ddagger}^{\ddagger} = 12.0$ kcal/mol in vacuo) leads by IRC to chlorides **5-CI** and **B** (see Scheme 2) in processes that approximate $S_{\text{N}}1$ reactions. The higher-energy TS (Figure 8b, $\Delta H_{\ddagger}^{\ddagger} = 19.6$ kcal/mol in vacuo), after IRC calculation, affords the same ion pair obtained from carbene **4** (Figure 7b).

The large energy gap (7.6 kcal/mol) between these two transition structures does not necessarily preclude competition from the higher-energy form because these results relate to computations carried out in vacuo. Attempts to determine the effects of solvation are limited to single-point calculations using simulated solvation PCM methodology. Upon application of single-point PCM calculations in simulated methanol, both transition-state energies were lowered, but the energy gap was not significantly altered. This method evaluates the overall effect of dielectric media on energies, but not specific solvation effects, e.g., hydrogen bonding, so it is likely that important differences could be overlooked.

Now, we can understand the disparity between the [5-OMe]/[5-Cl] product ratios from carbenes **3** and **4** (Figure 1). From carbene **4**, we obtain ion pair **12**. (Figure 7b, $\Delta H_{\ddagger}^{\ddagger} = 10.3$ kcal/mol in vacuo), which gives **5-OMe** and **5-Cl** by competitive reaction with either methanol or chloride. Carbene **3**, in contrast,

(32) Note that the polarized continuum model employed to optimize the ion pairs in *simulated* methanol does not use solvent molecules, and the model cannot speak to the molecular details of the solvent sheath surrounding the ion pair.

(33) For examples of “memory effects” in carbocation rearrangements, see Berson, J. A. *Angew. Chem., Int. Ed. Engl.* **1968**, *7*, 799.

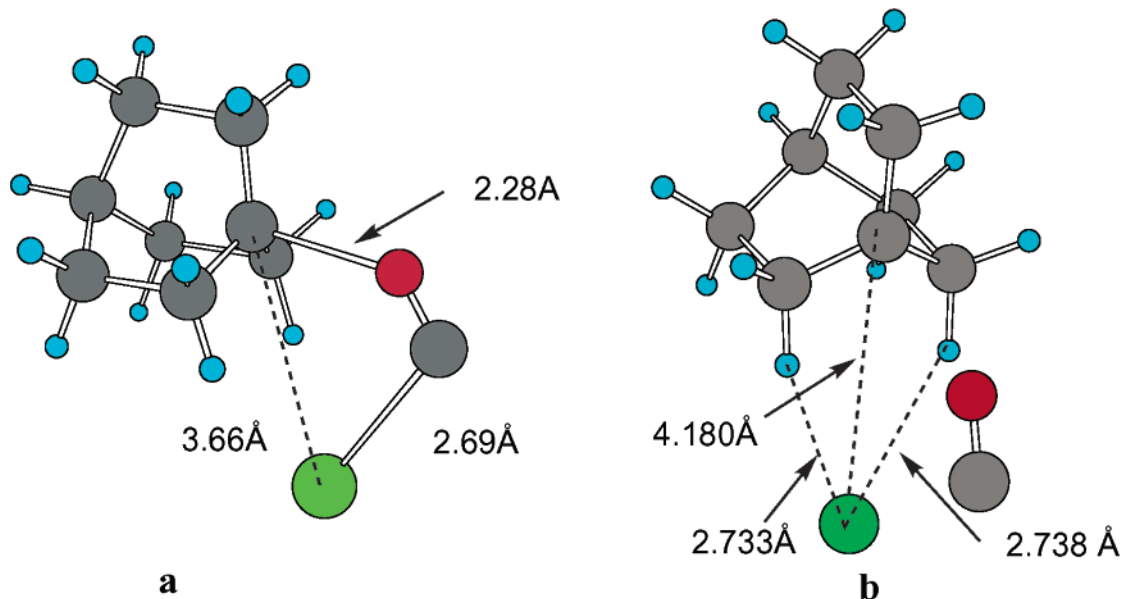


Figure 7. (a) B3LYP/6-31G(d) transition state for the fragmentation of carbene **4**. (b) Optimized ion pair from an IRC calculation on the TS shown in (a), using B3LYP/631G(d) in simulated methanol with the PCM.³⁰ See the Computational Methodology section in the Experimental Section.

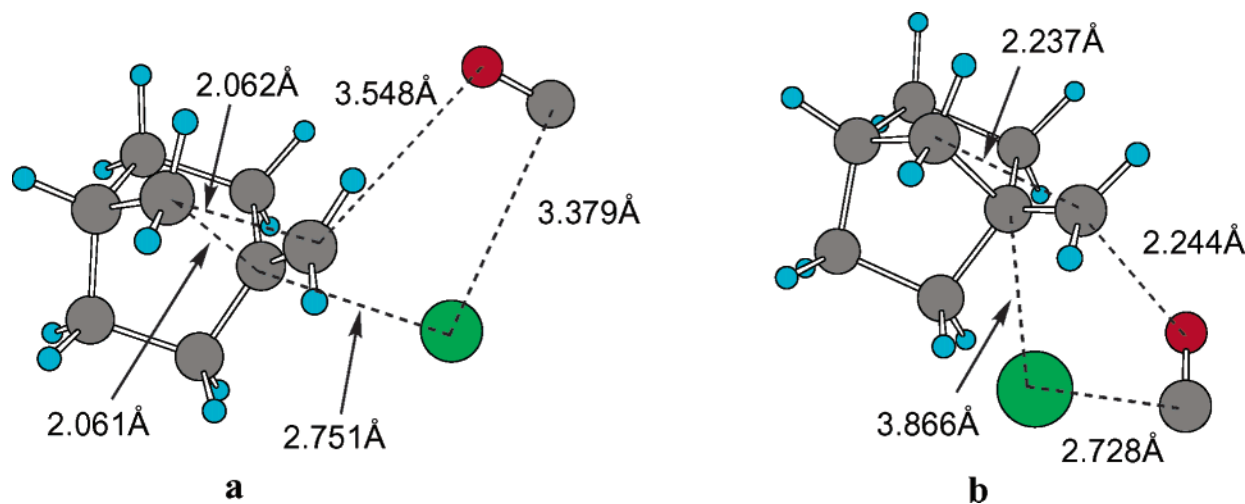
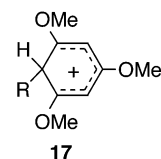


Figure 8. (a) Lower-energy B3LYP/6-31G(d) transition state for the ring expansion–fragmentation of carbene **3**, which leads to chlorides **5-Cl** and **B** (see Scheme 2). (b) Higher-energy TS for the ring expansion–fragmentation of carbene **3**, which leads to the ion pair of Figure 7b. See text and the Computational Methodology section of the Experimental Section.

mainly fragments to **5-Cl** by an $S_{\text{N}}1$ -like reaction via the TS of Figure 8a; little of this carbene fragments to ion pair **12** (Figure 8b). The computational study accords with the $[\text{5-OMe}]/[\text{5-Cl}]$ dependences on χ_{MeOH} shown in Figure 1. Carbene **4**, via ion pair **12**, leads to **5-OMe** or **5-Cl** in a ratio that is responsive to χ_{MeOH} , but carbene **3** mainly gives **5-Cl** by $S_{\text{N}}1$ fragmentation, no matter how much methanol is available.

Kinetics. Ion pair **16** (Figure 4b), formed from carbenes **9** or **10**, resembles an intimate or contact ion pair in the Winstein formulation.^{1,2} In MeOH/DCE, it can collapse to homoadamantyl chloride **11-Cl**, or evolve to a methanol-separated ion pair, from which solvent trapping generates ether **11-OMe**. However, at the solvent-separated ion pair stage, other trapping agents can compete for the homoadamantyl cation. For example, in the presence of 2.68 M trimethoxybenzene (TMB), laser flash photolytic (LFP) generation of carbene **9** in MeCN gives a UV signal for adduct **17** ($R = 3$ -homoadamantyl) at 385 nm.^{13,34}



We then carried out LFP experiments on solutions of 3-(1-adamantylmethoxy)-3-chlorodiazirine ($A_{356} = 1.0$) in MeCN containing 0.67–2.68 M TMB. In each case, we measured the absorbance of **17** at 385 nm. A Stern–Volmer analysis of $1/A_{17}$ vs $1/[\text{TMB}]$ was linear, and is shown in Figure 9. Assuming diffusion control for the reaction of the homoadamantyl cation (in **16**) with TMB, we can extract the cation lifetime from the intercept and slope of the Stern–Volmer correlation.^{34,35} The precision of the method, as applied to cation **16**, is not especially good: over nine experiments, τ ranged from $(0.72\text{--}5.87) \times 10^{-11}$ s, with an average value of 2.55×10^{-11} s.³⁶ We estimate

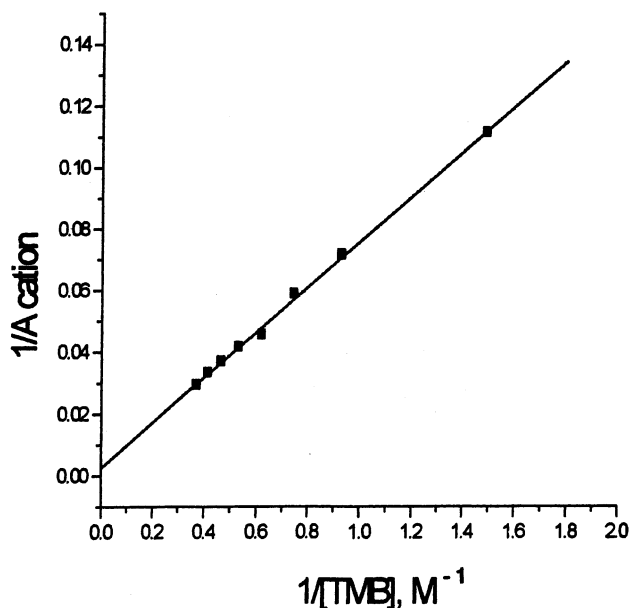


Figure 9. Stern–Volmer correlation of $1/\text{Absorbance}$ of cation **17** vs $1/[\text{TMB}]$ (M^{-1}); $r = 0.995$ for 8 points.

that the lifetime of the 3-homoadamantyl cation trappable by TMB in MeCN is ~ 20 – 30 ps.

It seems reasonable to identify the trappable cation as part of a solvent-separated ion pair derived from an intimate ion pair that resembles **16**. We note that the lifetime of the solvent-separated diphenylmethyl chloride ion pair is ~ 4.8 ns in MeCN,³ which is about 200 times longer than that of our homoadamantyl chloride ion pair. The longer lifetime of $[\text{Ph}_2\text{CH}^+//\text{Cl}^-]$ can be associated with the much greater stability of the diphenylmethyl cation, relative to the 3-homoadamantyl cation (9.2 kcal/mol in the gas phase).^{10a}

The polarities of MeCN ($\epsilon = 36.6$) and methanol ($\epsilon = 32.6$), as reflected by their dielectric constants, are similar. Therefore, we estimate that the time required for the evolution of the intimate homoadamantyl chloride ion pair to its solvent-separated form in MeOH/DCE is also on the order of 20 to 30 ps. This would be an upper limit to the time needed for solvent equilibration of the initial ion pairs generated from carbenes **9** or **10** (cf., Figures 4b and 5b). The 20–30-ps time interval is similar to the principal time constants for the main solvent relaxation processes of pure methanol (1, 39 ps)^{37a} and to the time constant (30.5 ps) for the reaction of diphenylmethyl cation with a methanol solvent shell.^{37b}

Solvent equilibration of the homoadamantyl chloride ion pair in methanol is in balance with ion pair decay, so that a modest

decrease in cation stability and lifetime (e.g., to the adamantyl cation) leads to the precursor-dependent, nonequibrated selectivity between chloride and methanol illustrated in Figure 2. On the other hand, we would predict that solvent-equilibrated ion pairs should be formed with cations that are as stable or more stable than the homoadamantyl cation (i.e., when the cation has $\Delta\Delta G \geq 4$ kcal/mol relative to the 1-adamantyl cation in the gas phase^{10a}).

Conclusions. $[\text{R}^+ \text{OC} \text{Cl}^-]$ ion pairs **12**, **14**, and **16** were generated, with R^+ as the 1-bicyclo[2.2.2]octyl, 1-adamantyl, or 3-homoadamantyl cation. The ion pairs were produced by either the direct fragmentation of alkoxychlorocarbenes ROCCl, with $\text{R} = 1$ -bicyclo[2.2.2]octyl, 1-adamantyl, or 3-homoadamantyl, or by the ring expansion–fragmentation of $\text{R}'\text{CH}_2\text{OCCl}$, with $\text{R}' = 1$ -norbornyl, 3-noradamantyl, or 1-adamantyl. Ion pairs were generated in methanol/dichloroethane solutions containing varying quantities of methanol, and gave ROME and RCl products by methanol capture or chloride return. From correlations of the $[\text{ROME}]/[\text{RCl}]$ product ratios as a function of methanol mole fraction, the homoadamantyl chloride ion pairs produced either by the direct fragmentation of 3-homoadamantylchlorocarbene or by the ring expansion–fragmentation of 1-adamantylmethoxychlorocarbene were identical. These ion pairs were solvent- and anion-equilibrated, and they were independent of precursor identity. LFP experiments involving a trimethoxybenzene cation trap afforded an estimate of 20–30 ps as the time required for solvent equilibration and “precursor amnesia.” This interval was also associated with the evolution of intimate to solvent-separated ion pairs in the Winstein solvolysis scenario.

In contrast, the methanol/chloride selectivities of the less-stable 1-adamantyl chloride and 1-bicyclo[2.2.2]octyl chloride ion pairs were not independent of their ROCCl or $\text{R}'\text{CH}_2\text{OCCl}$ carbene precursors. These ion pairs (especially when generated by ring expansion–fragmentation) were not solvent- and anion-equilibrated. Computational studies provided transition states for the carbene fragmentations and structures of the ion pairs. They also suggested that ring expansion–fragmentation of 1-norbornylmethoxychlorocarbene to 1-bicyclo[2.2.2]octyl chloride occurred via an S_{Ni} -like transition state, and largely bypassed the 1-bicyclo[2.2.2]octyl chloride ion pair.

Experimental Section

Isouronium salts. A. 1-Norbornylmethylisouronium Triflate. The general method of Moss et al.¹⁵ was employed. In a 50-mL round-bottom flask, equipped with a stirring bar and a reflux condenser protected with a calcium chloride tube, were placed 1.0 g (23.8 mmol) of cyanamide (NH_2CN), 3.0 g (23.8 mmol) of 1-norbornylmethanol,¹⁸ and 12 mL of anhydrous THF. To this solution was added 3.57 g (23.8 mmol) of trifluoromethanesulfonic acid. The mixture was magnetically stirred at 55 °C (oil bath) for 30 h. After the reaction mixture was cooled to room temperature, it was diluted with ether (200 mL) and kept in a refrigerator. White crystals of the isouronium salt (2.5 g, 70%) were filtered off, washed with cold ether (3×15 mL), and finally crystallized from acetone, mp 175–176 °C. ^1H NMR (δ , DMSO- d_6): 8.30 (br s, 4H, 2NH₂), 4.36 (s, 2H, CH₂O), 1.20–2.31 (m, 11H, norbornyl H).

Anal. Calcd for $\text{C}_{10}\text{H}_{17}\text{N}_2\text{F}_3\text{O}_4\text{S}$: C, 37.7; H, 5.4; N, 8.8. Found: C, 37.6; H, 5.1; N, 9.0.

B. 1-Bicyclo[2.2.2]octylisouronium Triflate. This material was prepared from 1-bicyclo[2.2.2]octanol^{18,19,21} using our standard method;¹⁵ see the detailed example above. We obtained 9–10% of the isouronium

- (34) For the visualization of carbocations by capture with TMB, see Pezacki, J. P.; Shukla, D.; Luszyk, J.; Warkentin, J. *J. Am. Chem. Soc.* **1999**, *121*, 6589. The operative form of the Stern–Volmer equation is $1/A_{\text{cat}} = k_o/(A_{\infty\text{cat}}k_{\text{TMB}}[\text{TMB}] + 1/A_{\infty\text{cat}})$, where A_{cat} is the absorbance of adduct **17** in the presence of various amounts of added TMB, $A_{\infty\text{cat}}$ is the absorbance of **17** at infinite [TMB], k_o is the sum of all the rate constants that lead to the disappearance of the homoadamantyl cation in the absence of TMB, and k_{TMB} is the bimolecular rate constant for the reaction of the homoadamantyl cation with TMB. Division of the intercept of the equation by its slope gives the value of k_{TMB}/k_o . Taking k_{TMB} as diffusion controlled gives k_o , and $1/k_o$ is τ , the lifetime of the homoadamantyl cation in ion pair **16**.
- (35) Platz, M. S.; Modarelli, D. A.; Morgan, S.; White, W. R.; Mullins, M.; Celebi, S.; Toscano, J. P. *Prog. React. Kinet.* **1994**, *19*, 93.
- (36) Johnson, L. A. Ph.D. Dissertation, Rutgers University, New Brunswick, NJ, 2001.
- (37) (a) Asaki, M. L. T.; Redondo, A.; Zawodzinski, T. A.; Taylor, A. J. *J. Chem. Phys.* **2002**, *116*, 8469. (b) Peon, J.; Polshakov, D.; Kohler, B. *J. Am. Chem. Soc.* **2002**, *124*, 6428.

salt as an oily solid. ^1H NMR (δ , DMSO- d_6): 8.51 and 8.32 (br s, 2H each, 2NH₂), 1.40–1.76 (m, 13H, bicyclooctyl H). ^{13}C NMR (δ , DMSO- d_6): 160.9, 120.6 (q, $J = 319.7$ Hz, CF₃), 74.1, 33.7, 26.8, 24.6. A satisfactory analysis could not be obtained. The derived diazirine (see below) had an appropriate UV maximum at 352 nm (pentane) or 353 nm (DCE).

C. 3-Noradamantylmethylisouronium Triflate. This material was prepared from 3-noradamantylmethanol²² using our standard method;¹⁵ see the detailed example above. We obtained 60% of the isouronium salt, mp 156–157 °C. ^1H NMR (δ , DMSO- d_6): 8.41 (br s, 4H, 2NH₂), 4.22 (s, 2H, CH₂O), 1.5–2.30 (m, 13H, noradamantyl H). ^{13}C NMR (δ , DMSO- d_6): 162.1, 75.9, 48.4, 45.3, 40.6, 36.8, 34.8.

Anal. Calcd for C₁₂H₁₉N₂F₃O₄S: C, 41.9; H, 5.5. Found: C, 42.0; H, 5.5.

D. 1-Adamantylmethylisouronium Tosylate. This material was prepared from a mixture of commercial 1-adamantylcarbinol (20 g, 0.12 mol), cyanamide (5.0 g, 0.12 mol), and anhydrous *p*-toluenesulfonic acid (from 22.8 g of the monohydrate, dried at 90 °C for 12 h under high vacuum) in 250 mL of freshly dried THF. The mixture was stirred and heated at 60–65 °C for 5 days under a nitrogen atmosphere. After cooling, the solid residue was filtered, washed with THF, air-dried, and chromatographed over silica gel with 10:1 CHCl₃/MeOH as eluent. We obtained 63% of the desired isouronium salt; mp 229–231 °C. ^1H NMR (δ , DMSO- d_6): 8.40 (br s, 4H, 2NH₂); 7.09–7.49 (q, 4H, Ar), 3.79 (s, 2H, CH₂O), 2.27 (s, 3H, CH₃), 1.53–1.96 (m, 15H, adamantyl).

Anal. Calcd for C₁₉H₂₈N₂O₄S: C, 60.0; H, 7.4; N, 7.4. Found: C, 59.6; H, 7.4; N, 7.4.

E. 3-Homoadamantylisouronium Triflate. This material was prepared from 3-homoadamantanol¹⁴ using our standard method;¹⁵ see above. We obtained 10% of white crystals (recrystallized from ether); mp 198–200 °C. ^1H NMR (δ , DMSO- d_6): 8.30 (br s, 4H, 2NH₂), 1.20–2.31 (m, 17H, homoadamantyl).

Anal. Calcd for C₁₃H₂₁N₂F₃O₄S: C, 43.6; H, 5.9; N, 7.8. Found: C, 43.6; H, 5.9; N, 7.4.

N-Methanesulfonyloxy-O-1-adamantylisourea. A. 1-Adamantyl Cyanate. Potassium hydride (20.0 mL of a well-shaken 30-wt-% solution in mineral oil) and 75 mL of dry ether were cooled to 0 °C in a 500-mL flask. 1-Adamantanol (4.0 g, 27 mmol) was then added in small portions, with stirring. The flask was protected with a CaCl₂ tube, and the mixture was stirred for 12 h at 25 °C. After recooling to 0 °C, 3.9 g (37 mmol) of cyanogen bromide in 10 mL of ether was added dropwise via an addition funnel, and stirring was continued for 3 h at 25 °C. The resulting mixture was filtered through a fritted glass funnel. The filtrate displayed cyanate IR absorptions³⁸ at 2258 and 2262 cm⁻¹.

B. N-Hydroxy-O-1-adamantylisourea. Crystalline hydroxylamine³⁹ (1.0 g, 30 mmol) was dissolved in 10 mL of dry ether in a 250-mL flask. The ethereal adamantyl cyanate solution (prepared above) was added dropwise, with stirring, via an addition funnel, while maintaining a reaction temperature of 0 °C. Stirring was continued for 3 h at 25 °C. Filtration and a wash with cold ether gave 1.43 g (26% based on 1-adamantanol) of the desired *N*-hydroxy-*O*-1-adamantylisourea; mp 166–168 °C (recrystallized from MeOH). ^1H NMR (δ , DMSO- d_6): 8.21 (s, 1H, OH), 5.20 (s, 2H, 2NH), 1.56–2.09 (m, 15H, adamantyl).

Anal. Calcd for C₁₁H₁₈N₂O₂: C, 62.8; H, 8.6; N, 13.3. Found: C, 63.0; H, 8.4; N, 13.2.

C. N-Methanesulfonyloxy-O-adamantylisourea. The procedure is based on related methods in the literature.⁴⁰ To a stirred suspension of *N*-hydroxy-*O*-1-adamantylisourea (1.43 g, 6.8 mmol) in 20 mL of CH₂Cl₂ at 0 °C, was added 0.6 g (7.6 mmol) of pyridine. After 10 min, 0.86 g (7.6 mmol) of methanesulfonyl chloride was added dropwise

via an addition funnel. The mixture was protected from moisture and stirred for 12 h at 25 °C. It was then washed with 2 × 5 mL of water, 5 mL of 1 M phosphoric acid, and finally with 5 mL of brine. The organic phase was dried over anhydrous sodium sulfate, filtered, and stripped to give the title compound as a yellow solid, 1.86 (86%). A small portion was recrystallized from petroleum ether/acetone, mp 110 °C. ^1H NMR (δ , DMSO- d_6): 6.54 (s, 2H, 2NH), 3.12 (s, 3H, CH₃), 1.57–2.12 (m, 15H, adamantyl).

Anal. Calcd for C₁₂H₂₀N₂SO₄: C, 50.0; H, 6.9; N, 9.7. Found: C, 49.5; H, 7.0; N, 9.6.

Diazirines. The 3-alkoxy-3-chlorodiazirines were prepared from the isouronium or isourea precursors by oxidation with NaOCl (Graham's reaction).¹⁶ The preparation of 3-chloro-3-(1-norbornylmethoxy)-diazirine is presented as a representative example.

The 1-norbornylmethylisouronium triflate (1.0 g, 3.3 mmol), 3.5 g of LiCl in 50 mL of DMSO, and 50 mL of pentane were cooled to 20 °C and stirred magnetically in a 500-mL flask. Then 200 mL of 12% aqueous sodium hypochlorite ("pool chlorine"), saturated with NaCl, was slowly added. Stirring was continued for 15 min at 15 °C after addition was complete. The reaction mixture was transferred to a separatory funnel containing 150 mL of ice water, the aqueous phase was removed, and the pentane phase was washed twice with ~75 mL of ice water, and then dried for 2 h over CaCl₂ at 0 °C. The diazirine/pentane solution was purified by chromatography over silica gel, eluted with pentane. The pentane eluate was concentrated by rotary evaporation and the pentane was replaced by DCE. Residual pentane was then removed by rotary evaporation at 0 °C.

^1H NMR (δ , CDCl₃): 4.00 (s, 2H, CH₂O), 2.25 (m, 1H, H4), 1.16–2.10 (m, 10 H, norbornyl). UV (DCE): 351, 364 nm.

The other alkoxychlorodiazirines were synthesized similarly. They all exhibited UV maxima in the 350–370 nm region. Their DCE solutions were adjusted so that $A = 0.5$ – 1.0 at λ_{max} .

Photolysis of Diazirines. Preparative photolysis solutions of diazirines in DCE or in MeOH/DCE were photolyzed at 25 °C for 1 h with a focused Oriel UV lamp, $\lambda > 320$ nm (uranium glass filter). The products were analyzed by capillary GC, GC–MS, and NMR. The capillary GC analysis used a 30 m × 0.25 mm (o.d.) × 0.25 μ (i.d.) CP–Sil 5CB (100% dimethyl polysiloxane) column at 50 °C, programmed to 250 °C at 20 deg/min. Product identities were confirmed by GC and GC–MS comparisons to authentic samples.

Laser flash photolytic experiments employed a Lambda Physik COMPex model 120 XeF₂ excimer laser. For a description of the LFP system, see Moss et al.⁸ The system has been upgraded by the incorporation of a 150-W pulsed Xe monitoring lamp, replacing the previously used 1000-W Xe lamp.

Products. The products enumerated in Schemes 2–7 were identified by capillary GC, GC–MS, and NMR comparisons to authentic samples. References to literature preparations of these materials are given in the text. Exceptions include protoadamantyl methyl ether (Scheme 4, **G**), whose identity is assumed based on its GC–MS molecular ion; adamantylmethyl formate (Scheme 6, **N**), which was prepared from 1-adamantylmethanol and formic acid;²⁶ and 3-homoadamantyl methyl ether (Schemes 6 and 7, **11-OMe**) whose preparation is described here.⁴¹

Sodium methoxide (0.15 g, 3.4 mmol) was added to a solution of 0.30 g (1.6 mmol) of 3-homoadamantyl chloride²⁵ (**11-Cl**) in 10 mL of methanol. The solution was refluxed for 12 h, then cooled, diluted with 30 mL of ether, and washed with 3 × 30 mL of water. The organic phase was dried over anhydrous MgSO₄, concentrated, and chromatographed over silica gel using 80:20 hexane/ether as eluent. 3-Homoadamantyl methyl ether (**11-OMe**) was obtained as a colorless oil (0.25 g, 85%).

^1H NMR (δ , C₆D₆): 3.08 (s, 3H, CH₃), 1.94–1.96 (m, 1H), 1.81–1.85 (m, 6H), 1.70–1.74 (m, 4H), 1.55–1.60 (m, 2H), 1.35–1.40 (m,

(41) We thank Dr. Jingzhi Tian for this preparation.

(38) Kauer, J. C.; Henderson, W. W. *J. Am. Chem. Soc.* **1964**, *86*, 4732.

(39) Hurd, C. D. *Inorganic Synthesis*; New York: McGraw-Hill: 1939; Vol. 1, p 87.

(40) (a) Grigat, E.; Putter, R.; König, C. *Chem. Ber.* **1965**, *98*, 144. (b) Stafford, J. A.; Gonzales, S. S.; Barret, D. G.; Suh, E. M.; Feldman, P. L. *J. Org. Chem.* **1998**, *63*, 10040.

4H). ^{13}C NMR (δ , C_6D_6): 76.7, 48.4, 43.8, 38.2, 36.7, 36.6, 32.0, 30.5, 28.3. MS (m/e): 180 (M^+), 149, 109, 79, 67.

Computational Methodology. All structures were fully optimized by analytical gradient methods using the Gaussian98 and Gaussian03 suites,^{30a} as well as density functional (DFT) calculations at the 6-31G-(d) level, with the exchange potentials of Becke,^{30a,b} and the correlation functional of Lee, Yang, and Parr.^{30a,c} Activation energies were corrected for zero-point energy differences (ZPVE, unscaled) and thermal effects at 298.150 K. Vibrational analyses established the nature of all stationary points as either energy minima (no imaginary frequencies) or first-order saddle points (one imaginary frequency). Solvation simulations used PCM methodology.^{30a}

Acknowledgment. We are grateful to the National Science Foundation for financial support and to the National Center for Supercomputing Applications for allocation of computer time

on the IBM p series 690 (Grant CHE 030060). We thank Dr. X. Fu for technical assistance.

Supporting Information Available: Tables S1–S6 of product distributions for carbenes **3**, **4**, **6**, **7**, **9**, and **10** in MeOH/DCE, transition states for the fragmentations of carbenes **6** and **7** at B3LYP/6-31G(d) (Figure S1), and Cartesian coordinates, enthalpies, and energies, and (where appropriate) imaginary frequencies for all ground and transition states, and intermediates (ion pairs) computed in this study (23 pages, print/PDF). This material is available free of charge via the Internet at <http://pubs.acs.org>.

JA040146O